UPR pathway is required for *Arabidopsis thaliana* resistance to necrophic fungal pathogens.

Blanchard Cécile[1], Aimé Sébastien[1], Ducloy Amélie[2], Hichami Siham[1], Marianne Azzopardi[2], Cacas Jean-Luc[2] and Lamotte Olivier[1*]

[1]Agroécologie, INRAE, Institut Agro Dijon, CNRS, Univ. Bourgogne, Univ. Bourgogne Franche-Comté, DIJON, France

[2]Institut Jean-Pierre Bourgin, INRAE, AgroParisTech, Université Paris-Saclay, VERSAILLES, FRANCE.

*Corresponding author: olivier.lamotte@inrae.fr

Abstract

Necrotrophic fungi such as *Botrytis cinerea* and *Alternaria brassicicola* kill host plant cells to feed themselves on dead plant tissues. *B. cinerea* is responsible for the development of grey mould, while *A. brassicicola* triggers black spot disease, both contributing to significant agricultural losses worldwide. In this article, we have investigated the contribution of the Unfolded Protein Response (UPR) pathway in the resistance of the model plant *Arabidopsis thaliana* to these two fungi. This cellular signalling pathway serves as a cellular protective mechanism, enhancing the protein folding capacity of the endoplasmic reticulum (ER). It is activated in response to the accumulation of unfolded or misfolded proteins within the ER. Our data indicate that the main branch of the UPR, regulated by the proteins IRE1A and IRE1B, along with the transcription factor bZIP60, contribute to plant resistance to *B. cinerea* and *A. brassicicola*. The mutants *ire1a/ire1b* and *bzip60* are indeed more susceptible to both pathogens. It correlates with the accumulation of mRNAs coding active bZIP60 in response to *B. cinerea*. Futhermore, the ER Quality Control (ER-QC) system is transcriptionally activated in response to *B. cinerea,* and mutation in the genes coding two of its component, the co-chaperone proteins SDF2 and ERdj3B, result in increased susceptibility to Botrytis. Proteins that are misfolded or aberrant can be targeted for proteasomal degradation through the ER-associated degradation (ERAD) pathway, assisted by the AAA+-ATPase CDC48. We showed that mutants in the genes coding the three arabidopsis CDC48 isoforms are more resistant to *B. cinerea*. To understand the involvement of IRE1 proteins and bZIP60 in immunity against *B. cinerea*, we adopted an RT-qPCR approach. Our data indicate that neither the classical defence genes typically induced by *B. cinerea* (PR1, PDF1.2, ORA59, PAD3) nor the genes responsible for ER-induced cell death (NAC089, Cathepsin B1, B2 and B3) are regulated by the IRE1A/bZIP60 pathway. However, we have demonstrated that mRNA coding the NAC053/NTL4 transcription factor accumulates significantly in the *bzip60* mutant, in contrast to its closest homolog, NAC078/NTL11. Finally, both mutants *nac053* and *nac078* were more resistant to *B. cinerea* infection indicating that these transcription factors act as negative regulator of Arabidopsis defence against B. cinerea.

Introduction

The maintenance of protein homeostasis is one of the cornerstones of cellular functions. It involves the precise regulation of translation, the folding of newly synthesized proteins, their post-translational modifications, their trafficking within the cell, their neofunctionalization and their degradation (Dissmeyer et al., 2019). The endoplasmic reticulum (ER) plays crucial roles in these processes and support the synthesis of one third to a quarter of all nascent proteins in eukaryotic cells (Kumari and Brodsky, 2021). Environmental factors, such as pathogen infections, intensify the workload on the protein folding machinery. When the endoplasmic reticulum (ER) is unable to meet the cell's demand for protein folding capacity, unfolded or misfolded polypeptides accumulate within the ER lumen, leading to a proteotoxic stress known as ER stress, which turns on the Unfolded Protein Response (UPR) signalling pathway. UPR is a conserved mechanism across eukaryotic species and, in Arabidopsis, it relies on three bZIP transcription factors (TF) that are anchored in ER membranes and made soluble and active through two distinct mechanisms when ER stress occurs. The first mechanism is the non-conventional splicing of the mRNA coding bZIP60. It results in a shift in the open reading frame, leading to the translation of a protein without a transmembrane domain that reach the nucleus. This process depends on the ER transmembrane proteins IRE1A and IRE1B which have a ribonuclease activity (Deng *et al.*, 2011; Nagashima *et al.*, 2011). Additionally, IRE1 ribonuclease activity is required for ER client mRNA degradation, a process known as Regulated IRE1-dependant decay (RIDD; Mishiba *et al.*, 2013; Pastor-Cantizano *et al.*, 2020), which reduce the amount nascent polypeptides across ER membranes, thus preventing the accumulation of unfolded proteins in the ER lumen. The second mechanism involves bZIP17 and bZIP28 which are translocated to the Golgi where they undergo intramembrane proteolytic cleavage, releasing an active transcription factors that reach the nucleus (Che *et al.*, 2010; Liu *et al.*, 2007). The activation of bZIP TF induce the upregulation of UPR genes, such as those coding for chaperones and factors involved in the ER-quality control (ER-QC) system, increasing ER folding capacity. It includes calreticulin (CRT) and calnexin (CNX), as well as BIPs proteins and its interacting proteins SDF2 and ERdj3 (Strasser, 2018). When folding failed, mis-folded and aberrant proteins are directed to degradation pathways and translocated out of the ER and ubiquitinated for proteasomal degradation. This process called ER-associated degradation (ERAD) involves the HRD1 complex and the AAA+-ATPAse CDC48 (Strasser et al., 2018).

A plethora of environmental situations can activate UPR pathways in plants, including heat, salt, drought or pathogen attacks (Reyes-Impellizzeri and Moreno, 2021; Verchot and Pajerowska-Mukhtar, 2021). Among them, few data highlight the role of UPR in response to necrotrophic pathogens. For instance, it was demonstrated that inoculating *Nicotiana attenuata* with *Alternaria alternata* resulted in the activation of UPR. Conversely, when *IRE1* or *bZIP60* genes were silenced, the plants exhibited heightened susceptibility to the fungus (Xu *et al.*, 2019). Morevover, Samperna *et al.* (2021) showed that impairment of IRE1/bZIP60 pathway in Arabidopsis enhanced the plant susceptibility to Drechslera gigantea. Although diseases caused by the necrotrophic fungal pathogens *Botrytis cinerea* and *Alternaria brassicicola* rank among the most devastating plant diseases worldwide, no data exists on the role of UPR in response to these two necrotrophic pathogens. *Botrytis cinerea* leads to the development of grey mold in a wide range of agricultural crops, while *Alternaria brassicicola* causes black spot disease in Brassica species. Both pathogens have the ability to infect the plant model *Arabidopsis thaliana*, making it a valuable tool for unravelling the intricate signalling pathways involved in plant disease tolerance to these pathogens. Innate immunity in plants is orchestrated through signalling cascades involving key hormones like salicylic acid (SA), jasmonic acid (JA), and ethylene (ET), inducing significant modifications in gene expression that underlie enhanced

resistance (Bürger and Chory, 2019). The JA signalling pathway is commonly linked to the establishment of plant defence against necrotrophic fungus (Macioszek *et al.*, 2023). Arabidopsis mutants with impaired JA perception, production or signalling are notably vulnerable to *B. cinerea* or *A. brassisicola* (Thomma *et al.*, 1998; Ferrari *et al.*, 2003). SA is recognized as a pivotal hormone that initiates immune responses against biotrophic pathogens (Bürger and Chory, 2019) but SA mediated signalling has also been shown to be involved in resistance against *B. cinerea* in Arabidopsis (Ferrari *et al.*, 2003) or against *Alternaria solani* in potato (Brouwer *et al.*, 2020). For a comprehensive exploration of cellular signalling cascades and their intricate interactions, the induction of marker genes is a widely employed and established method. Cellular mechanisms regulating the induction of JA-dependent genes are frequently investigated through the measurement of the induction of genes such as PDF1.2 or ORA59, while PATHOGENESIS-RELATED-1 (PR1) serves as a marker gene for SA (Zander *et al.*, 2010). A typical response of plants facing necrotrophic pathogens is the production in Arabidopsis of the phytoalexin camalexin through SA or JA signalling pathways, depending on the invading pathogen (Nguyen *et al.*, 2022). The last step of camalexin synthesis is catalysed by the cytochrome P450 CYP71B15 (PAD3) which mRNA accumulation correlates with camalexin production (Glawischnig, 2007). Camalexin has been shown to be toxic for *B. cinerea* and *A. brassicicola* (Chassot *et al.*, 2008; Sellam *et al.*, 2007), and mutation in *pad3* results in enhanced susceptibility to both pathogens (Ferrari et al., 2003; Thomma et al., 1999). During infection process, necrotrophic pathogens secretes compounds that enable rapid host cell death and disease spreading. *B. cinerea* produces cell-death inducing proteins but also manipulate the plant regulated cell death to promote host cell death (Bi *et al.* 2023; Govrin and Levine, 2000).

In this study, we explored the activation of the UPR, ERQC and ERAD in *Arabidopsis thaliana* in response to necrotrophic pathogens, with a specific emphasis on *Botrytis cinerea*. The role of UPR was investigated using a reverse genetics approach coupled with targeted gene induction experiments.

Results

Canonical UPR signalling pathways are involved in Arabidopsis susceptibility to necrotrophic pathogens.

We evaluated the importance of UPR signalling pathways during Arabidopsis infection by the two necrotrophic fungi *B. cinerea* and *A. brassicicola*. For this, we tested the susceptibility of Arabidopsis lines mutated in the genes coding the canonical UPR regulators AtIRE1A, AtIRE1B, AtBZIP17, AtBZIP28 and AtBZIP60. To test the susceptibility of UPR mutants to *B. cinerea*, plant leaves were drop-inoculated with a solution of conidia and lesion diameters were measured after 3 days of infection. WT Col plants exhibit classical 5 mm-necrotic lesions as described previously (Zimmerli *et al.*, 2001). A decrease of 18 % in lesion diameter was observed in *atbzip17-1* mutants compared to WT plants. To the opposite, both double *atire1a-2/atire1b-4* and *atbzip60-3* were 17 % more susceptible to the infection than WT plants. However, *atbzip28-2* mutant is as susceptible as WT plants (Figure 1A, Supplemental Figure S1A). *A. brassicicola* susceptibility was assessed by placing drops of a spore solution on leaves and lesion diameter were measured after 5 days of infection. In WT Col plants, Alternaria induced a lesion of 2.5 mm in diameter. Both *atbzip17-1* and *atbzip28-2* mutations do not impact the lesion size induced by *A. brassicicola.* However, double *atire1a-2/atire1b-4* or *bzip60.3* mutations induced a 27 % or a 37 % increase of the lesion diameter induced by this fungal pathogen compared to WT infected plants, respectively (Figure 1B, Supplemental Figure S1B).

***AtbZIP60* is upregulated and spliced in response to *Botrytis cinerea*.**

To go a step further, we then focus on the interaction between *A. thaliana* and *B. cinerea*. We checked by RT-qPCR the accumulation of the mRNA coding *AtIRE1A, AtIRE1B, AtBZIP17, AtBZIP28* and *AtBZIP60* following plant infection. Either a solution of *B. cinerea* spores in PDB or PDB alone (mock) were sprayed on leaves and samples were collected after 16 h, 24 h, 48 h and 72 h post-infection (hpi). To validate our experimental infection protocol for qPCR analysis, we first checked the expression of the classical defence genes *AtPAD3*, *AtPR1*, *AtPDF1.2a* and *AtPLP2* known to be strongly induced following Botrytis infection (Chassot *et al.*, 2008; La Camera *et al.*, 2005; Ferrari *et al.*, 2003). As expected, all four mRNA strongly accumulate in response to *B. cinerea* (Supplemental Figure S2). As observed in Figure 2, both *AtIRE*1A and *AtIRE1B* mRNA were not differentially accumulated in response to *B. cinerea* compared to control. The same was observed for *AtbZIP17* and *AtbZIP28* mRNAs except a slight induction at 48 hpi. To the contrary, mRNA coding the two forms of *AtbZIP60* accumulated in response to *B. cinerea*. More precisely, unspliced *AtbZIP60* mRNA accumulation was induced at 16 and 24 hpi ($p<0.01$, $p<0.05$, respectively). Spliced *AtbZIP60* mRNA accumulated at 16, 24, 48 hpi ($p<0.05$) and 72 hpi ($p<0.1$).

ERQC is involved during *B. cinerea* infection

Among the different ERQC components, the ER luminal binding proteins BIP and its co-chaperones ERDJ3A/B and SDF2 are key players of the ERQC machinery. To confirm the induction of the UPR pathway in response to *B. cinerea*, we checked by RT-qPCR the accumulation of the mRNA coding these proteins in plants infected or not. In comparison to mock-treated plants, infection induced the accumulation of mRNA coding the three arabidopsis BIP isoforms, *BIP1* and *BIP2* being the most induced as early as 16 hpi where as *BIP3* accumulation is weaker and occurs later. *BIPs* expression is no longer observable 72 hpi (Figure 3A). Concerning BIP co-chaperones *ERDJ3A*, *ERDJ3B* and *SDF2*, they were induced at 24 hpi with a maximum induction at 48 hpi (Figure 3A). To investigate whether the ERQC is crucial during plant susceptibility to botrytis, we challenged *erdj3b-1* and *sf2-2* mutants (Nekrasov *et al.*, 2009) with a spore solution of Botrytis and lesion diameters were measured after 3 days. Both mutants were more susceptible to botrytis infection as indicated by the increase of 24 % and 18 % in lesion diameter observed in *erdj3b-1* and *sf2-2,* respectively, compared to WT plants (Figure 3B, Supplemental Figure S3).

Mutation in the genes coding the ERAD component AtCDC48 results in plant resistance to *B. cinerea*

Following ERQC control, mis folded proteins are retro-translocated out of the ER for proteasomal degradation, the so-called ER Associated Degradation (ERAD). The role of the AAA+-ATPAse CDC48 in ERAD has been described in animals and plants. In Arabidopsis, AtCD48 is likely to be encoded by 5 genes (Bègue *et al.*, 2017). AtCDC48A, B and C proteins are closely related to the human and yeast CDC48 with which they share approximately 90 % similarity. By contrast, AtCDC48D and E are more different and exhibit no conserved domains in their N and C-terminus (Bègue *et al.*, 2017; Copeland *et al.*, 2016). To determine which Arabidopsis isoforms could functionally substitute yeast CDC48 and be potentially involved in ERAD pathway in plants, we first performed a yeast functional complementation tests using the *Saccharomyces cerevisiae cdc48* mutant strains KFY189 and DBY2030. KFY189 is a temperature-sensitive mutant which does not grow at 37°C whereas DBY2030 is cold-sensitive and fail to grow at 16°C (Feiler *et al.*, 1995; Frölich *et al.*, 1991). Both strains were transformed with the yeast expression vector pDRGW-F1 containing either the cDNA coding AtCDC48A, B, C, D or E or with the empty vector alone. All strains grown at 30°C (Supplemental Fig.

S4A, C). *S. cerevisiae* KFY189 or DBY 2030 strains containing either AtCDC48A, AtCDC48B or AtCDC48C coding sequence are able to grow at 37°C or 16°C, respectively, contrary to empty vector-transformed strains (Supplemental Figure S4B, D). As previously described, AtCDC48A can complement both strains (Feiler *et al.*, 1995). To the contrary, AtCDC48D or AtCDC48E expression in KFY189 or DBY2030 strains can not rescue their susceptibility to heat or cold, respectively, indicating that AtCDC48D or AtCDC48E are not functionally related to CDC48 proteins (Supplemental Figure S4B, D). In consequence, we focused our Arabidopsis experiments on AtCDC48A, B and C. In response to *B. cinerea* infection, *AtCDC48A* and *AtCDC48B* mRNA accumulated 48 and 72 hpi whereas *AtCDC48C* mRNA is not differentially accumulated in plants treated or not with *B. cinerea* (Figure 4A). We used different *AtCDC48* mutants to evaluate the involvement of ERAD during the pathogenic interaction between *A. thaliana* and *B. cinerea*. *Cdc48a-4/muse8* is a partial loss of function EMS mutant and has been described previously (Copeland *et al.*, 2016). *Cdc48b3* (Gabi_104F08) and *cdc48b4* (Gabi_485G04) are knockout and knockdown TDNA mutants, respectively, in the *AtCDC48B* gene in which *AtCDC48B* mRNA is not detected or reduced (Supplemental Figure S5A). We also used two knockout TDNA mutants in the AtCDC48C gene (cdc48c2/Salk_102955C and cdc48c3/Salk_123409) that do not express *AtCDC48C* mRNA (Supplemental Fig. S5B). Compared to control WT plants, *cdc48a-4/muse8* was slightly more resistant to *B. cinerea* infection (Fig. 4B, Supplemental Figure S5D). The same phenotype was observed with *cdc48b-4.* However, *cdc48b-3* and *cdc48c-2* were even more resistant, whereas *cdc48c-3* exhibited the strongest resistance with a 37% reduction in lesion diameter induced by *B. cinerea*. Using the opportunity to obtain previously published material (Neihl *et al.*, 2012), we produced Arabidopsis lines overexpressing either AtCDC48B-WT or AtCDC48B mutated in its two ATPase sites (AtCDC48B^{E308QE581Q} further abbreviated AtCDC48B-QQ) under the control of a CaMV35S promoter, the former leading to a dominant negative line. We selected two lines for each construct that overexpressed the transgene (Supplemental Figure S5C). Upon challenged with *B. cinerea*, plants overexpressing AtCDC48B-QQ were more resistant to the infection whereas plants overexpressing AtCDC48B-WT were as susceptible as WT plants (Figure 4B, Supplemental Figure S5D). These data indicate that AtCDC48 protein activities are required to induce full susceptibility of Arabidopsis plant to *B. cinerea.*

Mutation in IRE1A-IRE1B/bZIP60 pathway do not impact neither the expression of Botrytis-induced defence genes nor the expression of ER-stress-induced plant cell death genes.

Following *B. cinerea* perception, plant cells activate a complex array of induced defence including a transcriptional reprogramming. Among the mRNA which strongly accumulate, one may cite classical defence markers such as PR1, PDF1.2a, ORA59, FRK1, PAD3, GSTF6 (Supplemental Figure S2; Chassot *et al.*, 2008 ; La Camera *et al.*, 2011 ; Pré *et al.*, 2008). We checked by qRT-PCR whether the induction of these genes can be modified in mutants *ire1a-2-ire1b-4* and *bzip60-3* which are hypersusceptible to *B. cinerea*. All the above-mentioned mRNA accumulated at 24 and 48 hpi in the WT col-0 plants in comparison to mock-treated plants, except for *PR1* which accumulation is detected only 48 hpi as previously published (La Camera *et al.*, 2011). However, neither double *ire1a-ire1b* nor *bzip60* mutations impacted the accumulation of these mRNAs in response to *B. cinerea* infection (Supplemental Figure S6).

Evidences have been accumulating that necrotrophic pathogens such as *B. cinerea* actively induce plant cell death for subsequent colonization of dead tissue (Bi *et al.,* 2023). To explain the greater susceptibility of *ire1a-2-ire1b-4* and *bzip60-3*, we hypothesized that ER stress-induced plant cell death (ERSID) could be over-induced. ERSID is at least controlled by the ANAC089 transcription factor (Yang *et al*., 2014) and the Cathepsin proteases (Cai *et al.*, 2018). Whereas *ANAC089* and *Cathepsin B1, B2, B3* mRNA were shown to accumulate during ERSID induced by tunicamycin (Yang *et*

al., 2014; Cai *et al.*, 2018), none of these mRNA differentially accumulate during *B. cinerea* infection in comparison to mock-treated plants. Furthermore, none of these mRNA differentially accumulate in double *ire1a-1b* and *bzip60* mutants either in mock or Botrytis-treated plants compared to WT plants (Supplemental Figure S7).

AtANAC053 mRNA strongly accumulates in *bzip60* mutant in response to *B. cinerea* infection.

Gladman *et al.* (2016) showed that the expression of proteasome stress regulon-encoding genes, including *AtCDC48A* gene, are controlled by two NAC transcription factors, AtANAC053 (AtNTL4) and AtNAC078 (AtNTL11) and we showed that *AtCDC48* mutants are more resistant to *B. cinerea* (Figure 4B) indicating that CDC48 are required to facilitate fungal infection. To explain the increased susceptibility of the mutants *ire1a-2-ire1b-4* and *bzip60-3* to Botrytis, we hypothesized that the mRNA encoding AtANAC053 and AtNAC078 would be more highly induced in these mutants. As observed in figure 5A *AtNAC053* mRNA does not accumulate at 24 hpi in WT and *ire1a-2-ire1b-4* plants treated with *B. cinerea* in comparison to mock-treated plants. However, it strongly accumulates in *bzip60-3*-infected plants in comparison to WT plants. At 48 hpi, *AtNAC053* mRNA is induced in WT infected-plants to the same extend as the one observed in *bzip60-3.* However, it's still not induced in *ire1a-2-ire1b-4* (Figure 5B). Regarding *AtNAC078* mRNA, it does not accumulate in response to *B. cinerea* infection in any of the genotype tested neither at 24 nor at 48 hpi. We then compared the expression of *AtCDC48* mRNAs in WT and *ire1a-2-ire1b-4* and *bzip60-3*. *AtCDC48A, B, C* are not differentially expressed in response to *B. cinerea* infection in both genotypes compared to WT infected plants at 24 or 48 hpi (Supplemental Figure S8). We then challenged *Atnac053-1* and *Atnac078-1* mutants with *B. cinerea* and compared the lesion size induced at 3 dpi to WT infected plants (Figure 5C, Supplemental Figure S9). The lesion diameter observed in both *Atnac053-1* and *Atnac078-1* is lower than in WT indicating that both mutants are more resistant to *B. cinerea*. These results indicate that *NAC053* mRNA accumulation depends on bZIP60 and that both NAC053 and NAC078 act as negative regulator of Arabidopsis defence toward *B. cinerea*.

Discussion

The plant UPR pathway plays important roles in plant interaction with various pathogens, such as bacteria, fungi or viruses (Jing and Wang, 2020; Verchot and Pajerowska-Mukhtar, 2021). However, our understanding of its specific role during plant infections caused by necrotrophic fungal pathogens remains incomplete. Here we present a study that identifies UPR pathway as a critical element in *Arabidopsis thaliana* resistance to two necrotrophic fungi, *Botrytis cinerea* and *Alternaria brassicicola*. The RT-qPCR results demonstrated that *B. cinerea* infection activated UPR pathways in WT plants. During infection, we observed an accumulation of mRNAs coding the 3 AtBIP isoforms, along with its co-chaperones AtSDF2.2 and AtERDJ3A/3B. Additionally, we detected an increase in the accumulation of mRNAs coding the transcription factor AtbZIP60, in both its spliced and unspliced forms. The importance of UPR has been confirmed by challenging plants mutated in the genes coding the canonical UPR regulators AtIRE1A/AtIRE1B, AtbZIP60, as well as those of RIP-UPR AtbZIP17 and AtbZIP28 with a spore solutions of *B. cinerea*. Mutation in the genes coding *AtIRE1A* and *AtIRE1B* or *AtbZIP60* results in a greater plant susceptibility to *B. cinerea.* Similar observations were made when these mutants were challenged with *Alternaria brassicicola* indicating that IRE1-bZIP60 pathway plays important role in limiting the growth of both pathogens. However, it's worth noting that mutation in

AtbZIP28 did not have a significant impact on the plant's susceptibility to these fungi. Overall, our findings support the hypothesis that the IRE1-bZIP60 branch is an important element in the establishment of plant immunity to necrotrophic pathogens. This is reinforced by previous research on *Nicotiana benthamiana*, where silencing of *NbbZIP60*, *NbIRE1a*, and *NbIRE1b* expression through a VIGS approach led to increased plant susceptibility to the necrotrophic fungus *Alternaria alternata* (Xu et al., 2019). Furthermore, infection of the double mutant *atbzip28-2-atbzip60-1* with *Drechslera gigantea*, a necrotrophic fungus causing eyespot disease in crop plants, leads to increase disease symptoms compared to WT plants in Arabidopsis (Samperna *et al.*, 2021). However, it is noteworthy to mention that neither the knock down *atbzip60.1* nor the double mutant *atbzip28-2-atbzip60-1* showed increased susceptibility when infected with *B. cinerea* (data not shown). The significance of the IRE1-bZIP60 branch of the UPR in controlling plant immunity is further demonstrated by the work of Tateda *et al.* (2008), who showed that silencing of *IRE1a/1b* or *bZIP60* resulted in disease symptoms in *Nicotiana tabacum* caused by the non-host bacterial pathogen *Pseudomonas cichorri*. Additionally, concerning the virulent bacteria *Pseudomonas syringae pv maculicola* ES4326, bacterial growth was substantially more pronounced in *atire1a/ire1b* or *atbzip60* infected mutants compared to the infected WT plants (Moreno *et al.*, 2012). It is must be pointed out that our study revealed distinct responses to *B. cinerea* and *A. Brassicicola* depending on the genotype tested. Notably, the *atbzip17* mutant demonstrated higher resistance to *B. cinerea* compared to WT plants, while it exhibited a similar level of infection as WT plants when exposed to *A. Brassicicola*. Studies demonstrating a role of bZIP17 during biotic stresses are scarce. One may cite the study of Li *et al.* (2022) where the silencing of both NbbZIP17/28 delayed Rice Stripe Virus infection and decreased the accumulation of viral RNA and proteins in *N. benthamiana*, indicating that RIP-UPR promotes virus development. However, in Arabidopsis infected with the *Plantago asiatica* mosaic virus, AtbZIP60 and AtbZIP17 acts synergistically to restrict viral infection (Gayral *et al.,* 2020). Understanding the role of AtbZIP17 during *B. cinerea* infection will need further investigations.

Activation of UPR leads to an increase of the ER folding capacity, preventing the excessive build-up of misfolded or aberrant proteins that may occur during stressful situations such as pathogen attacks. If protein folding attempts fail, proteins are translocated to the cytosol for proteasomal degradation in a process known as ER-associated degradation (ERAD). During ERAD, misfolded proteins are tagged with polyubiquitin chains and extracted from the ER membrane with the assistance of the CDC48 AAA+ATPase complex (Strasser *et al.*, 2018). The number of gene coding CDC48 protein in Arabidopsis genome is unclear (Begue *et al.*, 2017). Through yeast *cdc48* mutant complementation experiments, our findings unequivocally establish that among the candidates, only three genes - AtCDC48A (At3g09840), AtCDC48B (At3g53230), and AtCDC48C (At5g03340) - encode proteins that serve as orthologs of ScCDC48 (as demonstrated in our study; Feiler et al., 1995). Thus, the two closely related AAA+-ATPase proteins (At2g03670 and At3g01610), previously referred to as AtCDC48D and E, as reported by Begue *et al.* (2017) and Copeland *et al.* (2016), are not ScCDC48 orthologues and should not be categorized as CDC48 protein within the context of Arabidopsis.

An increase in the accumulation of *AtCDC48A* and *AtCDC48B* mRNA have been detected during *B. cinerea* infection. Interestingly, plants mutated in either *AtCDC48A*, *AtCD48B* or *AtCDC48C* genes are more resistance to *B. cinerea* infection. Furthermore, the overexpression of an inactive form of AtCDC48B (*eg* AtCDC48B^{QQ}) also results in an increased resistance phenotype toward Botrytis. The resistant phenotype of *atcdc48a-4* mutant to *B. cinerea* can be explained by a constitutive immune response characterized not only by the stronger accumulation of *PR2* mRNA in this mutant (Copeland *et al.*, 2016). Ao et *al.* (2021) have proposed a model to explain this autoimmune phenotype related to the role of AtCDC48A during plant pathogen interaction. AtCDC48A is recognized by the SFC^{SNIPER7} complex and targeted for proteasomal degradation. It results in the accumulation of the NLR SNC1 (and likely other NLR) which may serve to enhance defence to the virulent oomycete pathogen *H.*

arabidopsidis NOCO2. The existence of such a mechanism in the context of *B. cinerea* infection remains to be demonstrated. Regarding AtCDC48A paralogs, AtCDC48B and AtCDC48C, it is unlikely they have redundant functions with AtCDC48A. This is supported by the observations that mutation in each of the *AtCDC48* gene results in resistant phenotypes against *B. cinerea.* Nonetheless, mutations in *AtCDC48B* or *AtCDC48C* do not affect the resistance of Arabidopsis to *H. Arabidopsis* NOCO2 (Copeland *et al.*, 2016). However, the importance of the IRE1-bZIP60 pathway in basal resistance to *B. cinerea* infection is unlikely linked to CDC48 because *AtCDC48* mRNAs do not accumulate differentially in *atire1a/ire1b* or *atbzip60* genetic backgrounds. Understanding the involvement of each of the *AtCDC48* genes in plant immunity will necessitate additional in-depth investigations.

To identify potential mechanisms that play a role in the defence response against *B. cinerea* via the IRE1-bZIP60 pathway, we have undertaken a RT-qPCR approach. None of the tested genes had their activation altered in the *atire1a-2/atire1b-4* and *atbzip60-3.* It concerns the SA (*PR1*) and JA (*PDF1.2, ORA59*) responsive genes, indicating that the IRE1-bZIP60 pathway does not influence the expression of SA and JA-dependant gene expression in response to *B. cinerea* infection. However, we did not investigate the hypothesis whether SA or JA signalling pathways were necessary to regulate the activation of UPR pathways as observed in other studies. In tomato, JA treatment induced the expression of *BIP1* and tunicamycin-induced *BIP1* expression was strongly reduced in the JA signalling mutant *jai1* indicating that JA pathway plays a role in ER stress signalling (Czékus *et al.*, 2020). Similar observations were made in *N. attenuata* in which MeJA treatment induced the accumulation of mRNA coding chaperone proteins such as BIP, PDI, CNX and CRT as well as the spliced form of *bZIP60* mRNA (Xu *et al.*, 2019). Using JA-deficient and JA-insensitive plants, these authors have also shown that JA pathway control the induction of mRNA coding chaperone proteins in response to *A. alternata* infection.

In addition, our data indicate that *PAD3* gene, which encode a cytochrome P450 enzyme that catalyses the last step of camalexin biosynthesis is not regulated through UPR pathway. To the contrary, the *F6'H1* gene was found less induced in *N. attenuata* plants impaired in the IRE1-bZIP60 pathway during *A. alternata* infection (Xu *et al.*, 2019). It encodes the key enzyme which catalyzes the synthesis of scopoletin and scopolin, two phytoalexin previously shown to be crucial for *N. attenuata* resistance to *A. alternata*. These results indicate that the role of UPR in regulating plant resistance to one particular class of pathogen is different from one plant-pathogen interaction model to another.

Necrotrophic pathogens induce plant cell death to their own benefits either by secreting plant cell death inducers or by manipulating host regulated cell death (Bi et al., 2023; Govrin and Levine, 2000). Genes known to orchestrate ER stress-induced plant cell death (ERSID), such as *AtNAC089* or *CathepsinB*, are not induced after *B. cinerea* infection whereas these genes are up-regulated following plant treatment with the ER stress-inducing agent tunicamycin (Yang et al., 2014; Cai et al., 2018). These results indicate that ER stress occurring upon *B. cinerea* infection or tunicamycin does not induce the same signalling pathways. In addition, increased susceptibility of *atire1a-2/atire1b-4* and *atbzip60-3* to *B. cinerea* is unlikely the consequence of an increase ERSID phenomenon because *NAC089* or *Cathepsin B* genes are not upregulated in these mutant genotypes. Overall, our results suggest that ERSID controlled by NAC089 and CathepsinB is unlikely to be involved during Arabidopsis-*B. cinerea* interaction.

Our data indicate that in *bzip60* mutant infected with *B. cinerea*, the expression of NAC053/NTL4 is upregulated. Infected-*bzip60* mutant accumulates much more *NAC053* mRNA than WT plant and this accumulation occurs earlier in *bzip60* (at 24 hpi) than in WT plant (at 48 hpi). However, the expression of the NAC053 closest relative NAC078/NTL11 is not modulated by *B. cinerea* in any of the genotypes tested. Both transcription factors have been shown to control the expression of the proteasome stress regulon including *CDC48A* (Gladman *et al.*, 2016). Nevertheless, the expression of genes coding CDC48 A, B or C proteins are not modulated in botrytis-infected *bzip60*

mutant. Very surprisingly, results are different when using *ire1a-ire1b* double mutant. *NAC053* mRNA does not accumulate neither at 24 hpi nor at 48 hpi in this mutant infected with *B. cinerea* in comparison to WT plants in which *NAC053* accumulate at 48 hpi. NAC053 is anchored to the plasma membrane (Kim *et al.*, 2010) and activated following stress perception in a ROS-dependant mechanism (Lee *et al*., 2014). Once activated, NAC053 control ROS production through the activation of *AtRBOH* genes (Lee *et al.*, 2012). In our model, it is reasonable to suggest that a disturbance in ROS homeostasis is likely present in the *bzip60* mutant, whereas such a disturbance might not exist in the *ire1a/ire1b* mutant. Further research is necessary to substantiate this hypothesis.

Experimental procedures

Plant materials

A. thaliana seeds were grown on jiffy-7 pellets in a growth chamber under controlled conditions (10h light/14h dark, 22°C/18°C, 60–70% humidity, light intensity of 100 and 120 μE.m^{-2}.sec^{-1}). All the mutants used are listed in Supplemental table S1. To screen T-DNA homozygous plant mutants by PCR, genomic DNA was isolated using Phire Plant Direct PCR kit (Thermoscientific) and PCR was performed using primers pairs as indicated in Supplemental table S2.

Pathogen infection

Botrytis cinerea strain BMM (Zimmerli *et al.*, 2001) was grown 10 days on sterile V8 agar plate (50% Campbells original V8 juice (v/v), 0.5 % KH2PO4 (m/v), 1.5 % agar (m/v), pH6) at 20°C in the dark. Spores were harvested by scraping the plate with sterile milliQ water and filtered through sterile gaze. Infection tests are carried out by placing 6 µL of a solution of botrytis spores (5.10^4 spores.mL^{-1} diluted in quarter-strength Difco potato dextrose broth PDB) on 4 leaves of four weeks old plants. Lesion diameters were measured after 3 days. For qPCR analysis, plants were either sprayed with a spore solution ($2.5.10^5$ spores.mL^{-1}) or with quarter-strength PDB as described previously (La Camera *et al.*, 2011). For both experiments, the inoculated plants are placed in a tray closed with a transparent lid to maintain a high-humidity environment.

Alternaria brassicicola strain MIAE01824 was provided by Dr. Christian Steinberg (INRAe, Dijon, France) and grown 15-20 days on PDA medium (19 g.L^{-1}) supplemented with sucrose (20 g.L^{-1}) and $CaCO_3$ (30 g.L^{-1}) at 20°C in the dark. Spores were harvested by scraping the plate with sterile infection medium (GamborB5 medium, Duchefa), sucrose 10 mM, KH_2PO_4 10 mM) and filtered through sterile gaze. Four leaves of four weeks old plants were drop inoculated (6 µL) with a solution of 1.10^6 spores.mL^{-1} in infection medium. Inoculated plants are placed in a tray closed with a transparent lid to maintain a high-humidity environment and lesion diameters were scored after 4 days.

RNA extraction and RT-qPCR analysis

Inoculated and mock-treated leaves were harvested at different time points, flash frozen and finely grinded in liquid nitrogen. Total RNA extraction and DNAse treatment were performed using SV Total RNA Isolation System (Promega) as described by the manufacturer. RNA integrity was analysed on a 1% agarose gel and concentration was measured using a nanodrop system (Thermoscientific). RNA (500 ng) were retrotranscribed into cDNA (High-Capacity cDNA Reverse Transcription Kit, Thermoscientific) using random hexamer and 17-mer oligodT primers. mRNA accumulation was assessed by real-time qPCR (GoTaq® qPCR Master Mix, Promega) and expression values were normalized to the expression of plant genes *At4g26410* and *At3g01150* as previously described as a stable reference genes (Czechowski *et al.*, 2005). Levels of transcripts were calculated using efficiency-weighted $\Delta\Delta Cq^{\omega}$ method (Ganger *et al.*, 2017). All primers are listed in Supplemental table S3.

Statistical methods

For infection tests, significant differences from WT plant were determined by a Kruskal–Wallis one-way anova on ranks followed by a comparison with the Dunnett's method. For qPCR analysis, ΔCq^{ω} value from one infection time-point is compared to the data of the control condition at the same time point using by a one-way ANOVA followed by a Tukey HSD Test (Ganger *et al.*, 2017). Then, data are represented on the figures as fold induction to the control condition ($\Delta\Delta Cq^{\omega}$).

AtCDC48B cloning procedures and transgenic lines generation

Using the opportunity to obtain previously published material (Neihl *et al.*, 2012), we produced Arabidopsis lines overexpressing either AtCDC48B or AtCDC48B mutated in its two ATPase sites ($AtCDC48B^{E308QE581Q}$) under the control of a CaMV35S promoter. PDONR/Zeo containing either $AtCDC48B^{WT}$ or $AtCDC48B^{E308QE581Q}$ cDNA were kindly provided by Drs. Annette Niehl and Manfred Heinlein (IBMP, Strasbourg, France). pDNOR/Zeo were BP-recombined (Thermoscientific) in pB2GW7 vector (Karimi *et al.,* 2002) and resulting vectors were introduced in *Agrobacterium tumefaciens* strain GV3101. WT A. thaliana Columbia plants (N60,000, Eurasian Arabidopsis Stock Center) were transformed using the floral dipping method (Clough and Bent, 1998). T1 and T2 transgenic plants were grown on jiffy-7 pellets and selected using BASTA herbicide after 10 days of growth. To identify homozygous plants overexpressing $AtCDC48B^{WT}$ or $AtCDC48B^{E308QE581Q}$, seeds from T2 plants were surface-sterilized and sown on MS Agar plates (4.4 $g.L^{-1}$ of Duchefa MS powder M0222.0050, 1% sucrose, 10 mM MES, 1% agar pH 5.7) containing 50 µg/mL of glufosinate ammonium (Sigma-Aldrich). Expression of mRNA coding $AtCDC48B^{WT}$ or $AtCDC48B^{E308QE581Q}$ in transgenics plants were analysed by RT-qPCR using primers described in supplemental table S3.

Acknowledgments

We would like to thank all the people who provided us with invaluable assistance in carrying out this work and particularly Pr. Nathalie Leborgne-Castel, Dr. Mathieu Gayral, Dr. Stéphane Bourque and Pr. David Wendehenne for helpful discussions. Pr. Steven H Howell, Pr. Cyril Zipfel and Pr. Xin Li are kindly thanked for sharing Arabidopsis mutants with us, Dr Kai-Uwe Fröhlich for providing Yeast strains, and Dr. Christian Steinberg for giving us *Alternaria brassicicola* MIAE01824 strain.

References

Ao, K., Tong, M., Li, L., Lüdke, D., Lipka, V., Chen, S., Wiermer, M. and Li, X. (2021) SCFSNIPER7 controls protein turnover of unfoldase CDC48A to promote plant immunity. *New Phytologist*, **229**, 2795–2811.

Bègue, H., Jeandroz, S., Blanchard, C., Wendehenne, D. and Rosnoblet, C. (2017) Structure and functions of the chaperone-like p97/CDC48 in plants. *Biochimica et Biophysica Acta (BBA) - General Subjects*, **1861**, 3053–3060.

Bi, K., Liang, Y., Mengiste, T. and Sharon, A. (2023) Killing softly: a roadmap of Botrytis cinerea pathogenicity. *Trends Plant Sci*, **28**, 211–222.

Brouwer, S.M., Odilbekov, F., Burra, D.D., Lenman, M., Hedley, P.E., Grenville-Briggs, L., Alexandersson, E., Liljeroth, E. and Andreasson, E. (2020) Intact salicylic acid signalling is required for potato defence against the necrotrophic fungus Alternaria solani. *Plant Molecular Biology*, **104**, 1–19.

Bürger, M. and Chory, J. (2019) Stressed Out About Hormones: How Plants Orchestrate Immunity. *Cell Host & Microbe*, **26**, 163–172.

Cai, Y.-M., Yu, J., Ge, Y., Mironov, A. and Gallois, P. (2018) Two proteases with caspase-3-like activity, cathepsin B and proteasome, antagonistically control ER-stress-induced programmed cell death in Arabidopsis. *New Phytologist*, **218**, 1143–1155.

Chassot, C., Buchala, A., Schoonbeek, H., Métraux, J.-P. and Lamotte, O. (2008) Wounding of Arabidopsis leaves causes a powerful but transient protection against Botrytis infection. *The Plant Journal*, **55**, 555–567.

Che, P., Bussell, J.D., Zhou, W., Estavillo, G.M., Pogson, B.J. and Smith, S.M. (2010) Signaling from the Endoplasmic Reticulum Activates Brassinosteroid Signaling and Promotes Acclimation to Stress in Arabidopsis. *Science Signaling*, **3**, ra69–ra69.

Copeland, C., Woloshen, V., Huang, Y. and Li, X. (2016) AtCDC48A is involved in the turnover of an NLR immune receptor. *The Plant Journal*, **88**, 294–305.

Czechowski, T., Stitt, M., Altmann, T., Udvardi, M.K. and Scheible, W.-R. (2005) Genome-Wide Identification and Testing of Superior Reference Genes for Transcript Normalization in Arabidopsis. *Plant Physiology*, **139**, 5–17.

Czékus, Z., Csíkos, O., Ördög, A., Tari, I. and Poór, P. (2020) Effects of Jasmonic Acid in ER Stress and Unfolded Protein Response in Tomato Plants. *Biomolecules*, **10**.

Deng, Y., Humbert, S., Liu, J.-X., Srivastava, R., Rothstein, S.J. and Howell, S.H. (2011) Heat induces the splicing by IRE1 of a mRNA encoding a transcription factor involved in the unfolded protein response in Arabidopsis. *Proceedings of the National Academy of Sciences*, **108**, 7247–7252.

Dissmeyer, N., Coux, O., Rodriguez, M.S. and Barrio, R. (2019) PROTEOSTASIS: A European Network to Break Barriers and Integrate Science on Protein Homeostasis. *Trends in Biochemical Sciences*, **44**, 383–387.

Feiler, H.S., Desprez, T., Santoni, V., Kronenberger, J., Caboche, M. and Traas, J. (1995) The higher plant Arabidopsis thaliana encodes a functional CDC48 homologue which is highly expressed in dividing and expanding cells. *The EMBO Journal*, **14**, 5626–5637.

Ferrari, S., Plotnikova, J.M., De Lorenzo, G. and Ausubel, F.M. (2003) Arabidopsis local resistance to Botrytis cinerea involves salicylic acid and camalexin and requires EDS4 and PAD2, but not SID2, EDS5 or PAD4. *The Plant Journal*, **35**, 193–205.

Fröhlich, K.U., Fries, H.W., Rüdiger, M., Erdmann, R., Botstein, D. and Mecke, D. (1991) Yeast cell cycle protein CDC48p shows full-length homology to the mammalian protein VCP and is a member of a protein family involved in secretion, peroxisome formation, and gene expression. *Journal of Cell Biology*, **114**, 443–453.

Ganger, M.T., Dietz, G.D. and Ewing, S.J. (2017) A common base method for analysis of qPCR data and the application of simple blocking in qPCR experiments. *BMC Bioinformatics*, **18**, 534.

Gayral, M., Arias Gaguancela, O., Vasquez, E., Herath, V., Flores, F.J., Dickman, M.B. and Verchot, J. (2020) Multiple ER-to-nucleus stress signaling pathways are activated during Plantago asiatica mosaic virus and Turnip mosaic virus infection in Arabidopsis thaliana. *The Plant Journal*, **103**, 1233–1245.

Gladman, N.P., Marshall, R.S., Lee, K.-H. and Vierstra, R.D. (2016) The Proteasome Stress Regulon Is Controlled by a Pair of NAC Transcription Factors in Arabidopsis. *The Plant Cell*, **28**, 1279–1296.

Glawischnig, E. (2007) Camalexin. *Phytochemistry*, **68**, 401–406.

Govrin, E.M. and Levine, A. (2000) The hypersensitive response facilitates plant infection by the necrotrophic pathogen Botrytis cinerea. *Current Biology*, **10**, 751–757.

Jing, M. and Wang, Y. (2020) Plant Pathogens Utilize Effectors to Hijack the Host Endoplasmic Reticulum as Part of Their Infection Strategy. Engineering, 6, 500–504.

Kim, S.-G., Lee, S., Ryu, J. and Park, C.-M. (2010) Probing protein structural requirements for activation of membrane-bound NAC transcription factors in Arabidopsis and rice. *Plant Science*, **178**, 239–244.

Kumari, D. and Brodsky, J.L. (2021) The Targeting of Native Proteins to the Endoplasmic Reticulum-Associated Degradation (ERAD) Pathway: An Expanding Repertoire of Regulated Substrates. *Biomolecules*, **11**.

La Camera, S., Geoffroy, P., Samaha, H., Ndiaye, A., Rahim, G., Legrand, M. and Heitz, T. (2005) A pathogen-inducible patatin-like lipid acyl hydrolase facilitates fungal and bacterial host colonization in Arabidopsis. The Plant Journal, 44, 810–825.

La Camera, S., L'Haridon, F., Astier, J., Zander, M., Abou-Mansour, E., Page, G., Thurow, C., Wendehenne, D., Gatz, C., Métraux, JP and Lamotte, O. (2011) The glutaredoxin ATGRXS13 is required to facilitate Botrytis cinerea infection of Arabidopsis thaliana plants. *The Plant Journal*, **68**, 507–519.

Lee, S., Lee, H.-J., Huh, S.U., Paek, K.-H., Ha, J.-H. and Park, C.-M. (2014) The Arabidopsis NAC transcription factor NTL4 participates in a positive feedback loop that induces programmed cell death under heat stress conditions. *Plant Science*, **227**, 76–83.

Lee, S., Seo, P.J., Lee, H.-J. and Park, C.-M. (2012) A NAC transcription factor NTL4 promotes reactive oxygen species production during drought-induced leaf senescence in Arabidopsis. *The Plant Journal*, **70**, 831–844.

Li, C., Zhang, T., Liu, Y., et al. (2022) Rice stripe virus activates the bZIP17/28 branch of the unfolded protein response signalling pathway to promote viral infection. *Molecular Plant Pathology*, **23**, 447–458.

Liu, J.-X., Srivastava, R., Che, P. and Howell, S.H. (2007) An Endoplasmic Reticulum Stress Response in Arabidopsis Is Mediated by Proteolytic Processing and Nuclear Relocation of a Membrane-Associated Transcription Factor, bZIP28. *The Plant Cell*, **19**, 4111–4119.

Macioszek, V.K., Jęcz, T., Ciereszko, I. and Kononowicz, A.K. (2023) Jasmonic Acid as a Mediator in Plant Response to Necrotrophic Fungi. *Cells*, **12**.

Mishiba, K., Nagashima, Y., Suzuki, E., Hayashi, N., Ogata, Y., Shimada, Y. and Koizumi, N. (2013) Defects in IRE1 enhance cell death and fail to degrade mRNAs encoding secretory pathway proteins in the Arabidopsis unfolded protein response. *Proceedings of the National Academy of Sciences*, **110**, 5713–5718.

Moreno, A.A., Mukhtar, M.S., Blanco, F., et al. (2012) IRE1/bZIP60-Mediated Unfolded Protein Response Plays Distinct Roles in Plant Immunity and Abiotic Stress Responses. *PLOS ONE*, **7**, e31944.

Nagashima, Y., Mishiba, K., Suzuki, E., Shimada, Y., Iwata, Y. and Koizumi, N. (2011) Arabidopsis IRE1 catalyses unconventional splicing of bZIP60 mRNA to produce the active transcription factor. *Scientific Reports*, **1**, 29.

Nekrasov, V., Li, J., Batoux, M., et al. (2009) Control of the pattern-recognition receptor EFR by an ER protein complex in plant immunity. *The EMBO Journal*, **28**, 3428–3438.

Nguyen, N.H., Trotel-Aziz, P., Villaume, S., Rabenoelina, F., Clément, C., Baillieul, F. and Aziz, A. (2022) Priming of camalexin accumulation in induced systemic resistance by beneficial bacteria against Botrytis cinerea and Pseudomonas syringae pv. tomato DC3000. *Journal of Experimental Botany*, **73**, 3743–3757.

Niehl, A., Amari, K., Gereige, D., Brandner, K., Mély, Y. and Heinlein, M. (2012) Control of Tobacco mosaic virus Movement Protein Fate by CELL-DIVISION-CYCLE Protein48. *Plant Physiology*, **160**, 2093–2108.

Pastor-Cantizano, N., Ko, D.K., Angelos, E., Pu, Y. and Brandizzi, F. (2020) Functional Diversification of ER Stress Responses in Arabidopsis. *Trends Biochem Sci*, **45**, 123–136.

Pré, M., Atallah, M., Champion, A., De Vos, M., Pieterse, C.M.J. and Memelink, J. (2008) The AP2/ERF Domain Transcription Factor ORA59 Integrates Jasmonic Acid and Ethylene Signals in Plant Defense. *Plant Physiology*, **147**, 1347–1357.

Reyes-Impellizzeri, S. and Moreno, A.A. (2021) The Endoplasmic Reticulum Role in the Plant Response to Abiotic Stress. *Frontiers in Plant Science*, **12**. https://doi.org/10.3389/fpls.2021.755447

Samperna, S., Boari, A., Vurro, M., et al. (2021) Arabidopsis Defense against the Pathogenic Fungus Drechslera gigantea Is Dependent on the Integrity of the Unfolded Protein Response. *Biomolecules*, **11**. https://doi.org/10.3390/biom11020240

Sellam, A., Iacomi-Vasilescu, B., Hudhomme, P. and Simoneau, P. (2007) In vitro antifungal activity of brassinin, camalexin and two isothiocyanates against the crucifer pathogens Alternaria brassicicola and Alternaria brassicae. *Plant Pathology*, **56**, 296–301.

Strasser, R. (2018) Protein Quality Control in the Endoplasmic Reticulum of Plants. *Annu. Rev. Plant Biol.*, **69**, 147–172.

Tateda, C., Ozaki, R., Onodera, Y., Takahashi, Y., Yamaguchi, K., Berberich, T., Koizumi, N. and Kusano, T. (2008) NtbZIP60, an endoplasmic reticulum-localized transcription factor,

plays a role in the defense response against bacterial pathogens in Nicotiana tabacum. *Journal of Plant Research*, **121**, 603–611.

Thomma, B.P.H.J., Eggermont, K., Penninckx, I.A.M.A., Mauch-Mani, B., Vogelsang, R., Cammue, B.P.A. and Broekaert, W.F. (1998) Separate jasmonate-dependent and salicylate-dependent defense-response pathways in Arabidopsis are essential for resistance to distinct microbial pathogens. *Proceedings of the National Academy of Sciences*, **95**, 15107–15111.

Thomma, B.P.H.J., Nelissen, I., Eggermont, K. and Broekaert, W.F. (1999) Deficiency in phytoalexin production causes enhanced susceptibility of Arabidopsis thaliana to the fungus Alternaria brassicicola. *The Plant Journal*, **19**, 163–171.

Verchot, J. and Pajerowska-Mukhtar, K.M. (2021) UPR signaling at the nexus of plant viral, bacterial, and fungal defenses. *Current Opinion in Virology*, **47**, 9–17.

Xu, Z., Song, N., Ma, L. and Wu, J. (2019) IRE1-bZIP60 Pathway Is Required for Nicotiana attenuata Resistance to Fungal Pathogen Alternaria alternata. *Frontiers in Plant Science*, **10**. https://doi.org/10.3389/fpls.2019.00263

Yang, Z.-T., Wang, M.-J., Sun, Ling, et al. (2014) The Membrane-Associated Transcription Factor NAC089 Controls ER-Stress-Induced Programmed Cell Death in Plants. *PLOS GENETICS*, **10**.

Zimmerli, L., Métraux, J.P. and Mauch-Mani, B. (2001) beta-Aminobutyric acid-induced protection of Arabidopsis against the necrotrophic fungus Botrytis cinerea. *Plant Physiol*, **126**, 517–523.

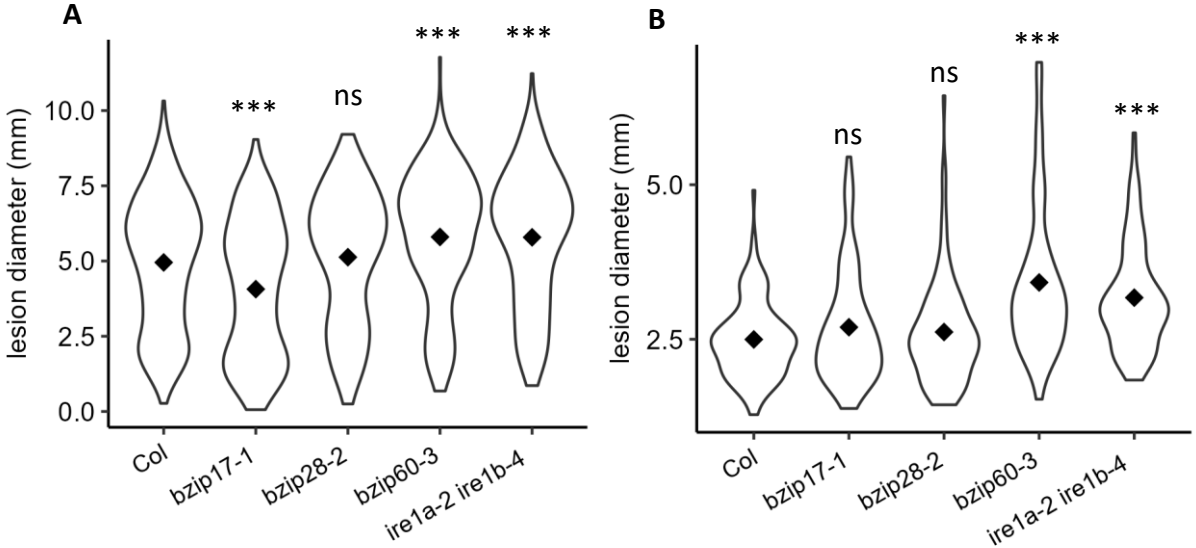

Figure 1 : Phenotype of *A. thaliana* UPR mutants infected with *B. cinerea* or *A. brassicicola*
Lesion diameters observed on wild-type (WT) Col and *upr* mutants were measured 3 days after *B. cinerea* infection (A) and 5 days after *A. brassicicola* infection (B). Experiments were repeated seven to eight times for *B. cinerea* infection depending on the genotype tested and four times for *A. brassicicola* infection. Seven plants per genotype were infected in each experiment. The stars indicate significant differences compared to the wild type and were identified using a Kruskal-Wallis' method followed by a Dunnett's test (*** $p < 0.001$; ns : no significant difference).

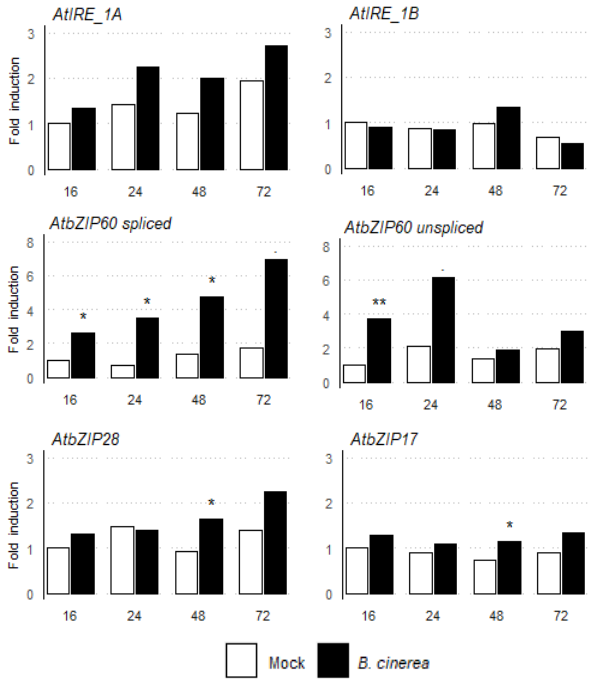

Figure 2 : mRNA accumulation of genes coding UPR main regulators after *B. cinerea* infection.
Plants were sprayed with ¼ PDB solution (Mock, white bars) or with ¼ PDB solution containing *B. cinerea* spores (black bars). Four leaves of three plants were collected at 16, 24, 48 and 72 hours post-inoculation. Level of transcripts coding IRE1A, IRE1B, bZIP17, bZIP28 and bZIP60 in its unspliced or spliced forms were quantified by RT-qPCR and normalized to the plant reference genes *AT4G26410* and *AT3G01150* transcript levels (Czechowski et al., 2005). Experiment were repeated five times and significant differences between non-infected and infected plants were determined by a one-way ANOVA followed by a Tukey HSD Test (*** $p<0.005$; ** $p<0.01$; * $p<0.05$; · $p<0.1$).

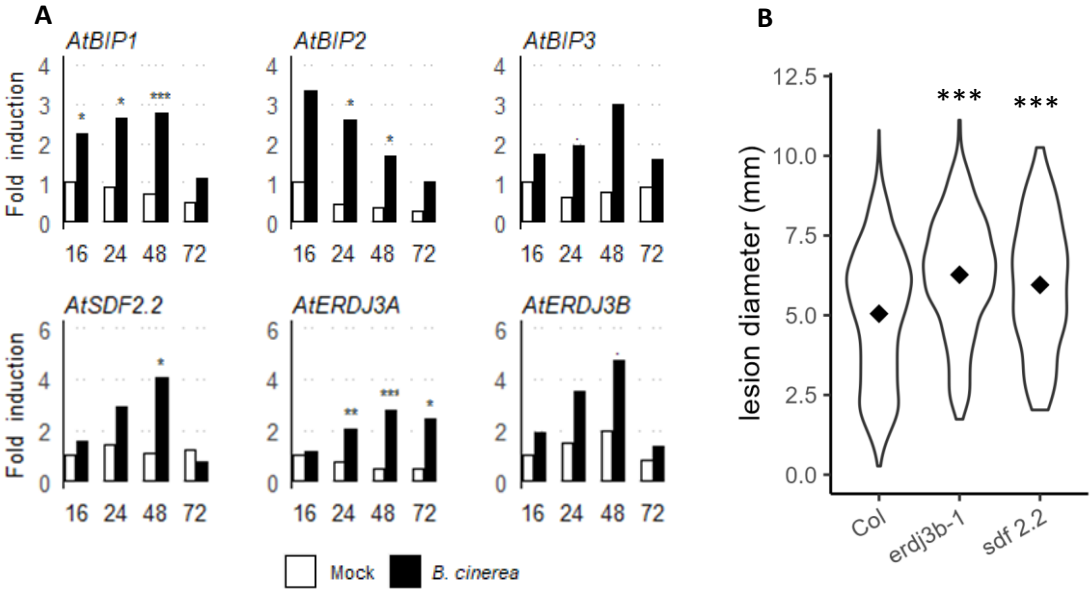

Figure 3 : Role of ERQC machinery during *B. cinerea* infection

(A) Accumulation of mRNA coding proteins involved in ERQC machinery in response to *B. cinerea* infection. Plants were sprayed with ¼ PDB solution (Mock, white bars) or with ¼ PDB solution containing *B. cinerea* spores (black bars). Four leaves of three plants were collected at 16, 24, 48 and 72 hours post-inoculation. Transcript levels were quantified by RT-qPCR and normalized to the plant reference genes *AT4G26410* and *AT3G01150* transcript levels (Czechowski et al., 2005). Experiment were repeated five times and significant differences between non-infected and infected plants were determined by a one-way ANOVA followed by a Tukey HSD Test (*** $p<0.005$; ** $p<0.01$; * $p<0.05$; · $p<0.1$).

(B) Phenotype of ERQC mutants infected by *B. cinerea*. Lesion diameters observed on wild-type (WT) Col and ERQC mutants were measured 3 days after *B. cinerea* infection. Experiments were repeated four times. Seven plants per genotype were infected in each experiment. The stars indicate significant differences compared to the wild type and were identified using Kruskal-Wallis' method followed by a Dunnett's test (*** $p < 0.005$; ns : non significant difference).

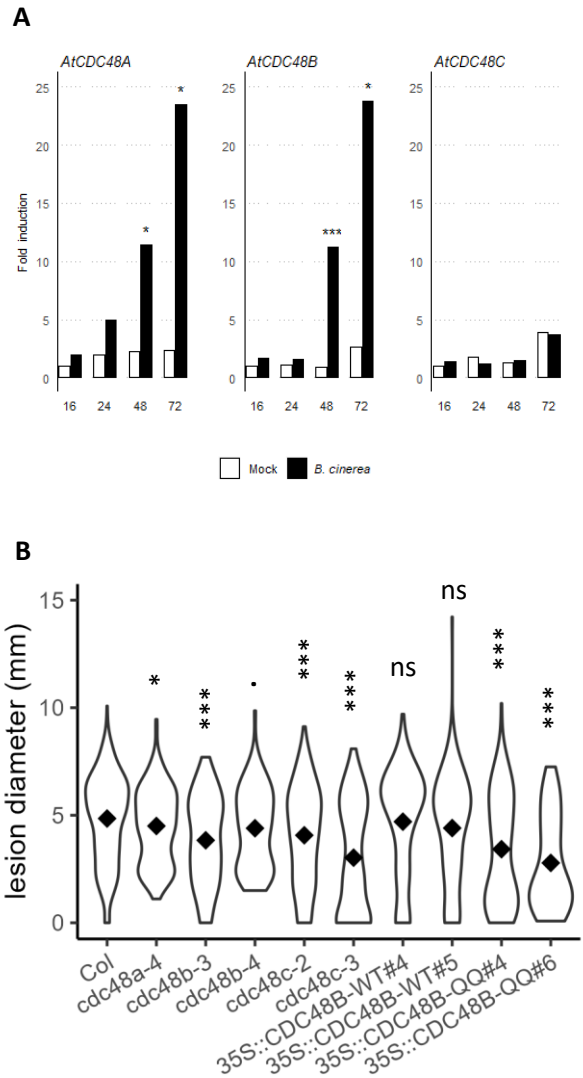

Figure 4 : Role of CDC48 proteins during *B. cinerea* infection

(A) Accumulation of mRNA coding CDC48A, CDC48B, CDC48C in response to *B. cinerea* infection. Plants were sprayed with ¼ PDB solution (Mock, white bars) or with ¼ PDB solution containing *B. cinerea* spores (black bars). Four leaves of three plants were collected at 16, 24, 48 and 72 hours post-inoculation. Transcript levels were quantified by RT-qPCR and normalized to the plant reference genes *AT4G26410* and *AT3G01150* transcript levels (Czechowski et al., 2005). Experiment were repeated five times and significant differences between non-infected and infected plants were determined by a one-way ANOVA followed by a Tukey HSD test (*** $p<0.005$; * $p<0.05$).

(B) Phenotype of CDC48 mutants and plants expressing a WT (CDC48B-WT) or an inactive isoforms of CDC48B (CDC48B-QQ) infected by *B. cinerea*. Lesion diameters observed on wild-type (WT) Col and mutants were measured 3 days after *B. cinerea* infection. Experiments were repeated seven to nine times. Seven plants per genotype were infected in each experiment. The stars indicate significant differences compared to the wild type and were identified using Kruskal-Wallis' method followed by a Dunnett's test (*** $p<0.005$; * $p<0.05$; · $p<0.1$).

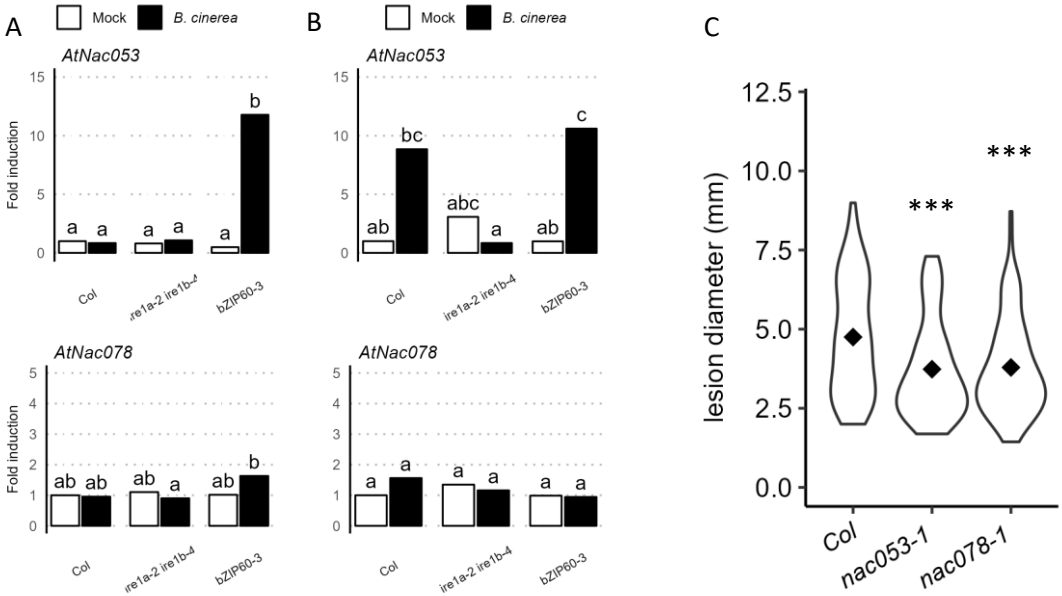

Figure 5 : Role of NAC053 and NAC078 during *B. cinerea* infection

(A-B) Accumulation of mRNA coding NAC053 and NAC078 in response to *B. cinerea* infection in WT, *ire1a/ire1b* and *bzip60* mutants. Plants were sprayed with ¼ PDB solution (Mock, white bars) or with ¼ PDB solution containing *B. cinerea* spores (black bars). Four leaves of three plants were collected at 24 h (A) or 48 h (B) post-treatment. Transcript levels were quantified by RT-qPCR and normalized to the plant reference genes *AT4G26410* and *AT3G01150* transcript levels (Czechowski et al., 2005). Experiments were repeated six times. Different letters represent groups which were significantly different from one another as determined by a one-way ANOVA followed by a multiple comparison with a Fisher's Least Significant Difference (LSD) test.

(C) Phenotype of *nac053* and *nac078* mutants infected with *B. cinerea*. Lesion diameters observed on wild-type (WT) Col and mutants were measured 3 days after *B. cinerea* infection. Experiments were repeated four times. Seven plants per genotype were infected in each experiment. The stars indicate significant differences compared to the wild type. Significant differences between a mutant genotype and WT plants were tested using Kruskal-Wallis' method followed by a Dunnett's test (*** $p < 0.005$; ns : non significant difference).

Supp FigS1

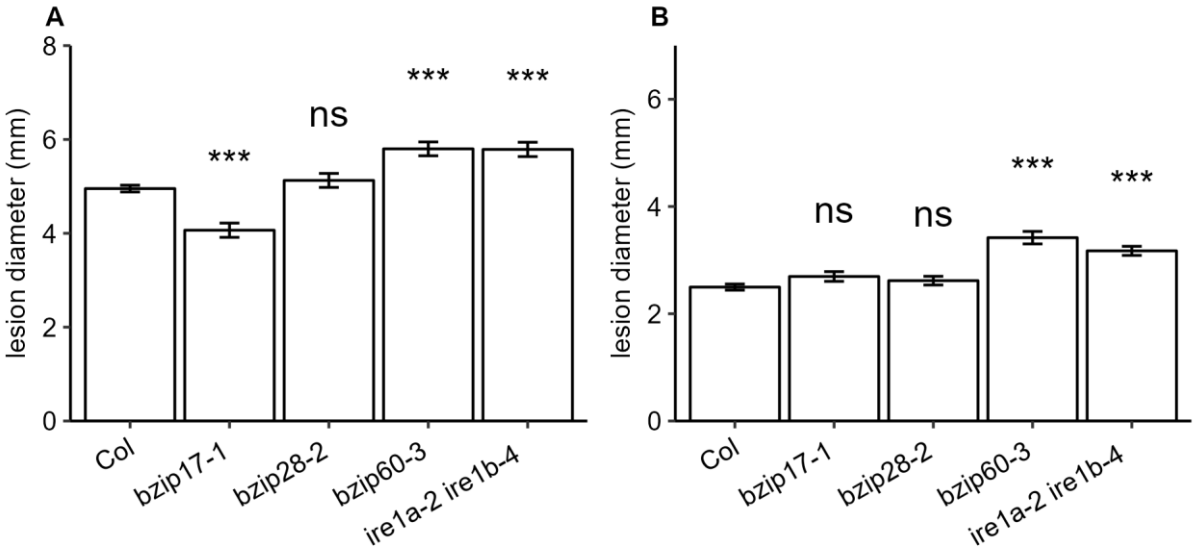

Supplemental Figure S1 : Phenotype of *A. thaliana* UPR mutants infected with *B. cinerea* or *A. brassicicola*

Lesion diameters observed on wild-type (WT) Col and *upr* mutants were measured 3 days after *B. cinerea* infection (A) and 5 days after *A. brassicicola* infection (B). Experiments were repeated seven to eight times for *B. cinerea* infection depending on the genotype tested and four times for *A. brassisicola* infection. Seven plants per genotype were infected in each experiment. The stars indicate significant differences compared to the wild type which were identified using a Kruskal-Wallis' method followed by a Dunnett's test (*** $p < 0.005$; ns : non significant difference).

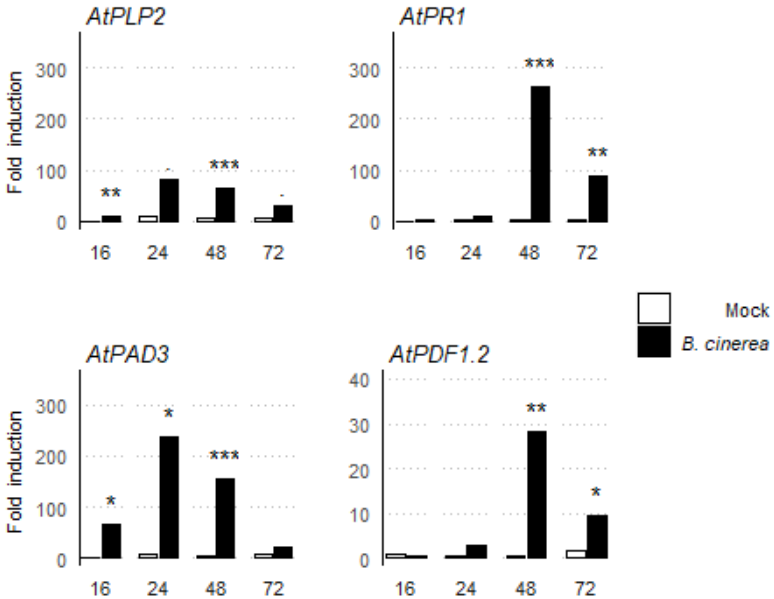

Supplemental Figure S2: Accumulation of mRNA coding PLP2, PR1, PAD3 and PDF1.2 in response to *B. cinerea* infection in our experimental conditions.

Plants were sprayed with ¼ PDB solution (Mock, white bars) or with ¼ PDB solution containing *B. cinerea* spores (black bars). Four leaves of three plants were collected at 16, 24, 48 and 72 hours post-inoculation. Transcript levels were quantified by RT-qPCR and normalized to the plant reference genes AT4G26410 and AT3G01150 transcript levels (Czechowski et al., 2005). Experiment were repeated five times and significant differences between non-infected and infected plants were determined by a one-way ANOVA followed by a Tukey HSD test (*** $p<0.005$; ** $p<0.01$; * $p<0.05$; · $p<0.1$).

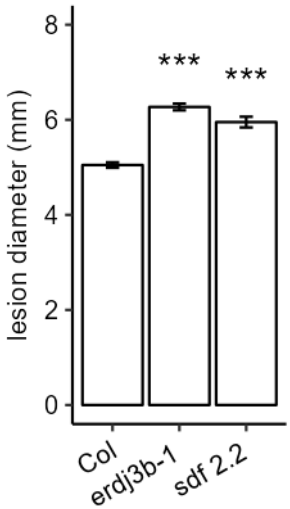

Supplemental Figure S3: Phenotype of ERQC mutants infected by B. cinerea.
Lesion diameters observed on wild-type (WT) Col and ERQC mutants were measured 3 days after *B. cinerea* infection. Experiments were repeated three to four times. Seven plants per genotype were infected in each experiment. The stars indicate significant differences compared to the wild type and were identified using Kruskal-Wallis' method followed by a Dunnett's test (*** $p < 0.005$; ns : non significant difference).

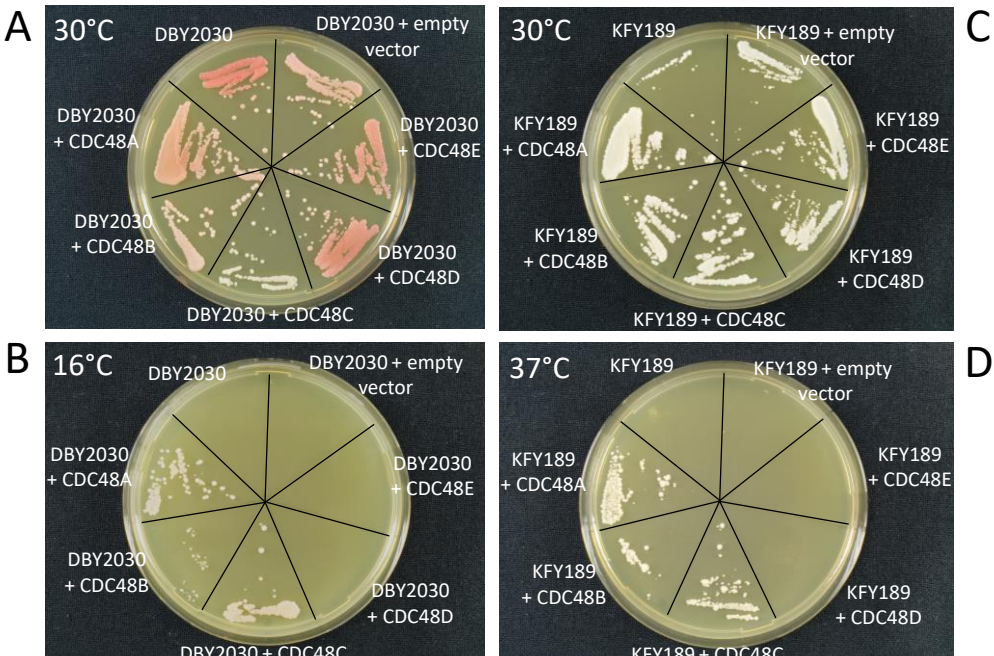

Supplemental Figure S4: Functional complementation of yeast cdc48 mutants.
The yeast CDC48 mutant strains which are cold sensitive (strain DBY2030) or temperature sensitive (strain KFY189) were transformed with pDRF1GW vector containing or not cDNA coding Arabidopsis CDC48 proteins. Yeast strains were then streaked out on YDP agar plate and grown at 30°C (A, C) or 16°C for DBY2030 (B) or 37°C for KFY189 (D). Experiments were repeated three times with similar results.

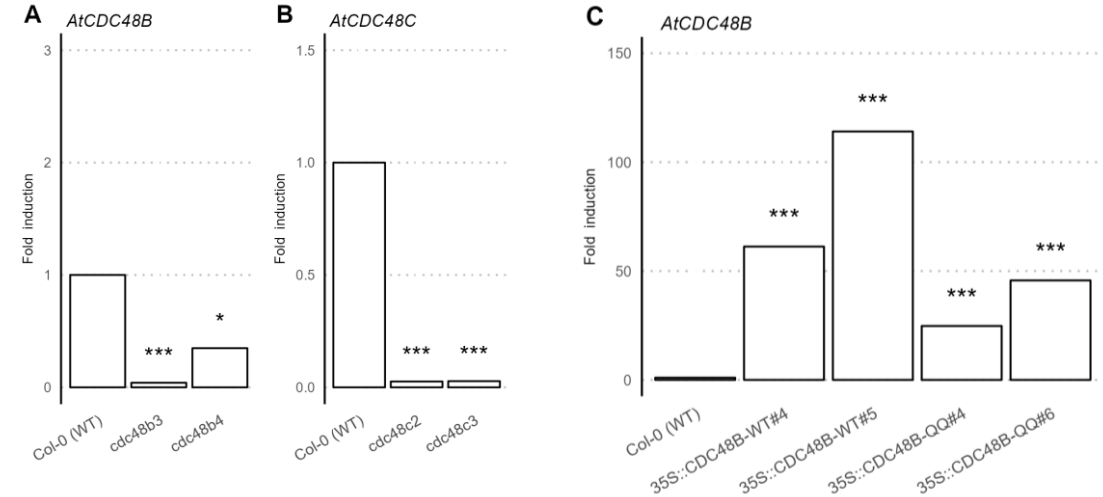

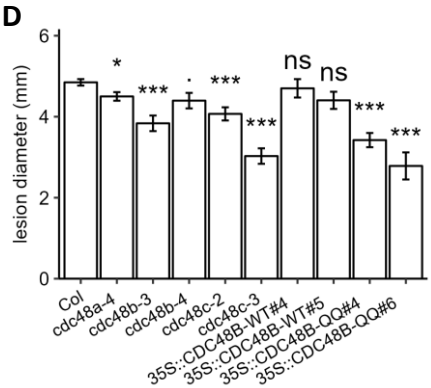

Supplemental Figure S5: Expression of CDC48 in *cdc48* mutants and phenotype of these mutants lines infected with *B. cinerea.*

A, B, C. Expression of CDC48 mRNAs in *cdc48b* and *cdc48c* mutants and in CDC48B overexpressing lines. Four leaves of three plants were collected and *CDC48B* or *CDC48C* transcript levels were quantified by RTqPCR in *cdc48b3* and *cdc48b4* (A) or in *cdc48c2* and *cdc48c3* (B) mutants, respectively. AtCDC48B transcript level was quantified in transgenic lines overexpressing CDC48B-WT or CDC48B^{E308QE581Q} (CDC48-QQ). All transcript level were normalized to the plant reference genes AT4G26410 and AT3G01150 transcript levels (Czechowski et al., 2005). Experiment were repeated five times and significant differences between non-infected and infected plants were determined by a one-way ANOVA followed by a Tukey HSD test (*** $p<0.005$).

D. Phenotype of CDC48 mutants and plants expressing a WT (CDC48B-WT) or an inactive isoforms of CDC48B (CDC48B-QQ) infected by *B. cinerea*. Lesion diameters observed on wild-type (WT) Col and mutants were measured 3 days after *B. cinerea* infection. Experiments were repeated seven to nine times. Seven plants per genotype were infected in each experiment. The stars indicate significant differences compared to the wild type which were identified using Kruskal-Wallis' method followed by a Dunnett's test (*** $p<0.005$; * $p<0.05$; · $p<0.1$).

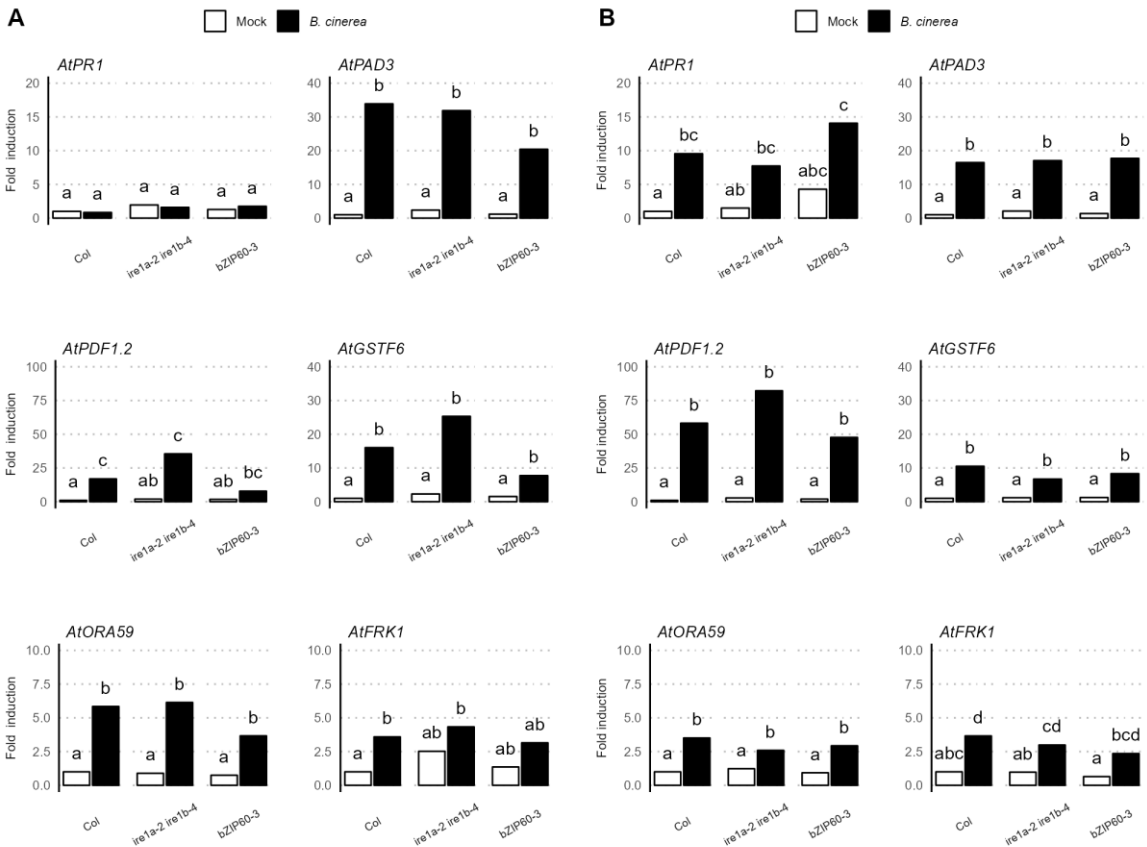

Supplemental Figure S6 : Accumulation of mRNA coding classical defense genes in response to *B. cinerea* infection in WT, *ire1a/ire1b* and *bzip60* mutants.

Plants were sprayed with ¼ PDB solution (Mock, white bars) or with ¼ PDB solution containing *B. cinerea* spores (black bars). Four leaves of three plants were collected at 24 h (A) or 48 h (B) post-treatment. Transcript levels were quantified by RT-qPCR and normalized to the plant reference genes *AT4G26410* and *AT3G01150* transcript levels (Czechowski et al., 2005). Experiments were repeated six times. Different letters represent groups which were significantly different from one another as determined by a one-way ANOVA followed by a multiple comparison with a Fisher's Least Significant Difference (LSD) test.

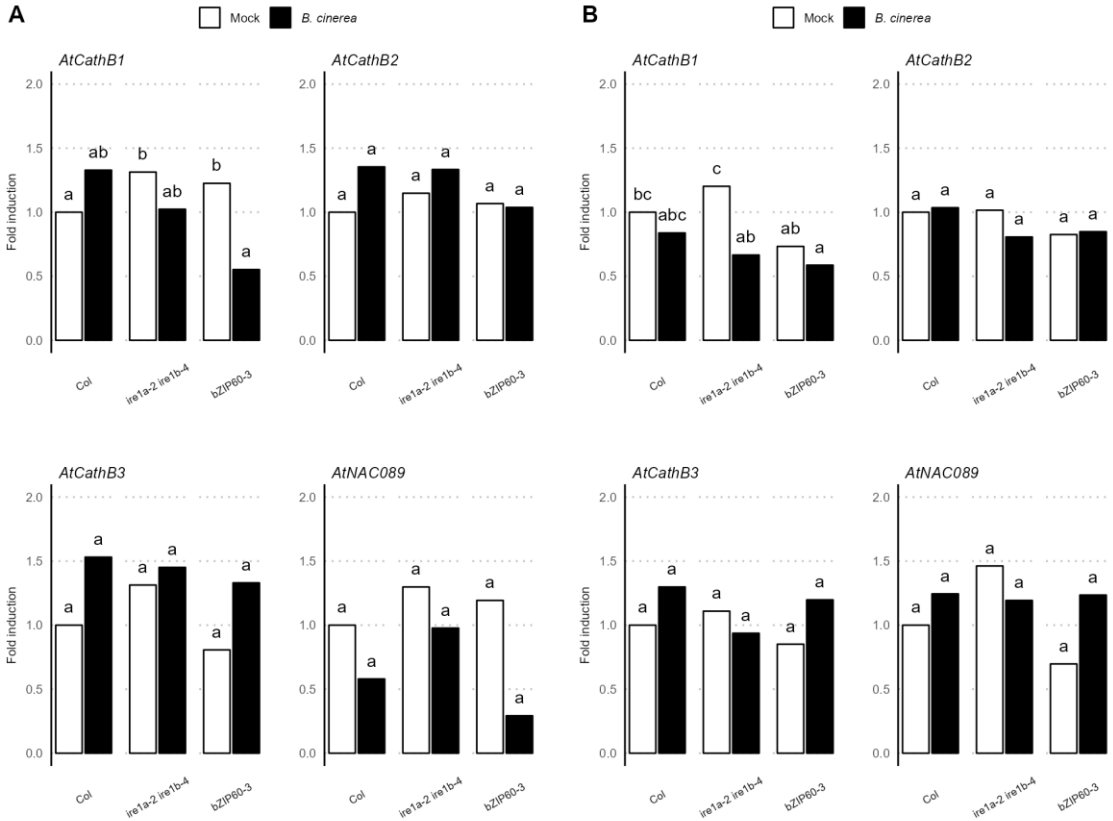

Supplemental Figure S7 : Accumulation of mRNA coding cathepsin and NAC089 transcription factor in response to *B. cinerea* infection in WT, *ire1a/ire1b* and *bzip60* mutants.

Plants were sprayed with ¼ PDB solution (Mock, white bars) or with ¼ PDB solution containing *B. cinerea* spores (black bars). Four leaves of three plants were collected at 24 h (A) or 48 h (B) post-treatment. Transcript levels were quantified by RT-qPCR and normalized to the plant reference genes *AT4G26410* and *AT3G01150* transcript levels (Czechowski et al., 2005). Experiments were repeated six times. Different letters represent groups which were significantly different from one another as determined by a one-way ANOVA followed by a multiple comparison with a Fisher's Least Significant Difference (LSD) test.

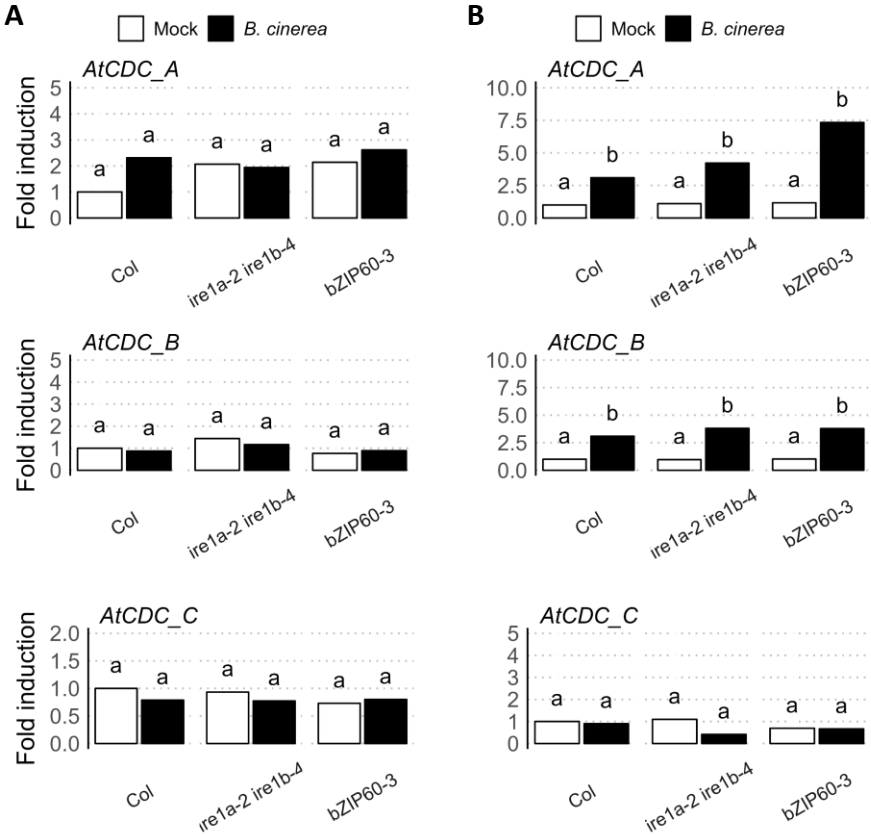

Supplemental Figure S8 : Accumulation of mRNA coding CDC48 in response to *B. cinerea* infection in WT, *ire1a/ire1b* and *bzip60* mutants.

Plants were sprayed with ¼ PDB solution (Mock, white bars) or with ¼ PDB solution containing *B. cinerea* spores (black bars). Four leaves of three plants were collected at 24 h (A) or 48 h (B) post-treatment. Transcript levels were quantified by RT-qPCR and normalized to the plant reference genes *AT4G26410* and *AT3G01150* transcript levels (Czechowski et al., 2005). Experiments were repeated six times. Different letters represent groups which were significantly different from one another as determined by a one-way ANOVA followed by a multiple comparison with a Fisher's Least Significant Difference (LSD) test.

Blanchard *et al.*

Supplementary methods:

CDC48 expression in *cdc48* yeast mutant

CDC48 cDNA were cloned from an Arabidopsis thaliana cDNA pools made from total RNA extracted from Arabidopsis Col-0 plants. AtCDC48A (At3g09840; forward primer ATGTCTACCCCAGCTGAATCTTC; reverse primer CTAATTGTAGAGATCATCATCGTCCC), AtCDC48C (At5g03340; forward primer ATGTCAAACGAACCGGAATC; reverse primer CTAACTGTAGAGATCGTCGTCATC), AtCDC48D (At2g03670; forward primer ATGTTGGAAACCGAAAGC; reverse primer TCATGTAGCAGAAGCTACTAGTAA), AtCDC48E (At3g01610; forward primer ATGGGGAGGAGAGGTCGC; reverse primer TTACTCGAGGGTAAAAGATGGCC) were amplified by PCR using Phusion DNA polymerase (Thermoscientific) and cloned into PCR8 vector (Thermoscientific). PDONR/Zeo containing either CDC48B (At3g53230) was kindly provided by Drs. Annette Niehl and Manfred Heinlein (Niehl *et al.*, 2012; Institut de biologie moléculaire des plantes, Strasbourg, France). PCR8 and pDNOR/Zeo vectors were then recombined in pDRF1-GW (Loque *et al.,* 2007) and resulting vectors or empty vector were introduced in *cdc48* deficient *Saccharomyces cerevisiae.* Two *cdc48 S. cerevisiae* mutants were kindly provided by K.-U. Fröhlich (University of Graz, Austria): the cold-sensitive strain DBY2030 (MATa ade2-101 lys2-801 ura3-52 cdc48-1; Frolich *et al.*, 1991) or the temperature-sensitive strain KFY189 (MATa lys2 leu2 ura3 cdc48-8). Transformed *S. cerevisiae* cells were plated on minimal selective medium containing 2% glucose, 0,77g/L SD-URA drop out mix (Clontech), 0.67 g/L Yeast Nitrogen Base (Sigma-Aldrich), 15 g/L agar (Sigma-Aldrich) and grown at 30°C. Transformed colonies were checked by colony PCR and then grown overnight at 30°C under shaking in YPD medium (10 g/L yeast extract, 20 g/L peptone, 2% glucose). Yeast cells were then streaked out on YDP agar plate (YPD medium containing 15g/L agar) and grown at 30°C and 16 °C for DBY2030 transformed strain or 30°C and 37°C for KFY189 transformed strain.

References:

Fröhlich KU, Fries HW, Rüdiger M, Erdmann R, Botstein D, Mecke D (1991) Yeast cell cycle protein CDC48p shows full-length homology to the mammalian protein VCP and is a member of a protein family involved in secretion, peroxisome formation, and gene expression. J. Cell Biol. 114: 443-453. https://doi.org/10.1083/jcb.114.3.443

Loqué D, Lalonde S, Looger LL, von Wirén N, Frommer WB (2007) A cytosolic trans-activation domain essential for ammonium uptake. Nature. 446: 195-198. https://doi.org/10.1038/nature05579

Niehl A, Amari K, Gereige D, Brandner K, Mély Y, Heinlein M (2012) Control of *Tobacco mosaic virus* Movement Protein Fate by CELL-DIVISION-CYCLE Protein48, *Plant Physiology* 160: 2093-2108. https://doi.org/10.1104/pp.112.207399

Wallis JW, Chrebet G, Brodsky G, Rolfe M, Rothstein R (1989) A hyper-recombination mutation in *S. cerevisiae* identifies a novel eukaryotic topoisomerase. Cell 58: 409-419. https://doi.org/10.1016/0092-8674(89)90855-6

Supplemental table S1 : list of mutants used in this study

mutant name	gene locus	mutant reference	references	origin	
Atbzip17-1	At2g40950	SALK_104326	Liu et al., 2007a	Pr. Steven H Howell	https://doi.org/10.1111/j.1365-313X.2007.03195.x
Atbzip28-2	At3g10800	SALK_132285C	Liu et al., 2007b	Pr. Steven H Howell	https://doi.org/10.1105/tpc.106.050021
Atbzip60-3	At1g42990	GABI_326A12	Bao et al., 2012	Pr. Steven H Howell	https://doi.org/10.1080/15548627.2018.1462426
Atire1a-2	At2g17520	SALK_018112	Deng et al., 2011	Pr. Steven H Howell	https://doi.org/10.1073/pnas.1102117108
Atire1b-4	At5g24360	SAIL_238_F07	Deng et al., 2011	Pr. Steven H Howell	https://doi.org/10.1073/pnas.1102117108
Atire1a-2/Atire1b-4		SALK_018112 x SAIL_238_F07	Moreno et al., 2012	Pr. Steven H Howell	https://doi.org/10.1371/journal.pone.0031944
Aterdj3b-1	At3g62600	SALK_113364	Nekrasov et al, 2009	Pr. Cyril Zipfel	https://doi.org/10.1038/emboj.2009.262
Atsdf2.2	At2g25110	SALK_141321	Nekrasov et al, 2009	Pr. Cyril Zipfel	https://doi.org/10.1038/emboj.2009.262
Atcdc48a-4/muse8	At3g09840	EMS mutant	Copeland et al., 2016	Pr. Xin Li	https://doi.org/10.1111/tpj.13251
Atcdc48b-3	At3g53230	Gabi_104F08	our study	NASC	
Atcdc48b-4	At3g53230	Gabi_485G04	our study	NASC	
Atcdc48c-2	At5g03340	SALK_102955C	our study	NASC	
Atcdc48c-3	At5g03340	SALK_123409	our study	NASC	
Atnac53-1	At3g10500	SALK_009578C	Gladman et al., 2016	NASC	https://doi.org/10.1105/tpc.15.01022
Atnac78-1	At5g04410	SALK_025098	Gladman et al., 2016	NASC	https://doi.org/10.1105/tpc.15.01022

NASC : Nottingham Arabidopsis Stock Centre (https://arabidopsis.info/)

Supplemental table S2 : Primers used for mutant genotyping

mutant name	line	LB primer name	LB primer sequence	gene specific primer 1	gene specific primer 2
Atcdc48b1	GABI_104F08	GABI-LB-o8474	ATAATAACGCTGCGGACATCTACATTTT	TTCTCATCCCTCCTCTAACTAGGA	TAAATATGAACACCGAGCTCCTCA
Atcdc48b2	GABI_485G04	GABI-LB-o8474	ATAATAACGCTGCGGACATCTACATTTT	TTCTCATCCCTCCTCTAACTAGGA	TAAATATGAACACCGAGCTCCTCA
Atcdc48c1	SALK_123409	Lbe	GGAACAACACTCAACCCTATCTCG	GGTTGCTCTCACTCTCACCAG	TATGTCAAACGAACCGGAATC
Atcdc48c2	SALK_102955C	Lbe	GGAACAACACTCAACCCTATCTCG	GGTTGCTCTCACTCTCACCAG	TATGTCAAACGAACCGGAATC
Atnac053-1	SALK_009578C	Lbe	GGAACAACACTCAACCCTATCTCG	TCAAGAAGCAAACATGTGGTG	GATGACGACGCTTCTTTTCAG
Atnac078-1	SALK_025098	Lbe	GGAACAACACTCAACCCTATCTCG	TCTTTCGCATTTGCGATATTC	TTCAAGTTCTGGTTTTCACCG
Atbzip17-1	SALK_104326	Lbe	GGAACAACACTCAACCCTATCTCG	AAGGAGCAGCCTCCTCCAC	GCCTTTCTCGAAGCCACGG

Supplemental table S2 : RT-qPCR primers used in this work

name	locus		RT-qPCR primers	ref	
AtCDC48A	At3g09840	forward	AAACTCGAATTCTCTACTTTTT	CDC48 A	this work
		reverse	TTTTTCCATTTGTAATGAACGACC		
AtCDC48B	At3g53230	forward	GGTTGTGGATGAAGCCATTA	CDC48 B	this work
		reverse	CGGTTCCCATACTTGACATCAG		
AtCDC48C	At5g03340	forward	GGCGATACAATTCTCATCAAC	CDC48 C	this work
		reverse	GACGGGGCATTCTTCTCAGC		
reference gene	*At4g26410*	forward	GAGCTGAAGTGGCTTCCATGAC	Czechowski *et al.* , 2005	https://doi.org/10.1104/pp.105.063743
		reverse	GGTCCGACATACCCATGATCC		
reference gene	*At3g01150*	forward	GATCTGAATGTTAAGGCTTTTAGCG	Czechowski *et al.* , 2005	https://doi.org/10.1104/pp.105.063743
		reverse	GGCTTAGATCAGGAAGTGTATAGTCTCTG		
AtIRE1A	AT2G17520	forward	GCTTCAGACCTCATATCCCG	Afrin *et al.* , 2020	https://doi.org/10.1038/s41598-020-76114-1
		reverse	AGCATCACGAAGGAAAGACAG		
AtIRE1B	AT5G24360	forward	GGTGGGATGAGAAACTGGATA	Afrin *et al.* , 2020	https://doi.org/10.1038/s41598-020-76114-1
		reverse	AGTTTGTTCCGTATGACCCG		
AtBzip60	AT1G42990	forward	GGAGACGATGATGCTGTGGCT	Afrin *et al.* , 2020	https://doi.org/10.1038/s41598-020-76114-1
AtBzip60 unspliced Rev		reverse	CAGGGATTCCAACAAGAGCACAG		
AtBzip60 spliced Rev		reverse	CAGGGAACCCAACAGCAGACT		
AtbZIP28	AT3G10800	forward	GCCAGTGATCCTCTCTTTGC	Qiang *et al.* , 2012	https://doi.org/10.1105/tpc.111.093260
		reverse	CAGAAGACAGTGCACCAGGA		
AtbZIP17	AT2G40950	forward	ACAGGAGATCGGGAGAGGAT	Qiang *et al.* , 2012	https://doi.org/10.1105/tpc.111.093260
		reverse	GCTCCTCGACGTAATGCTTC		
AtBIP1	AT5G28540	forward	GCTCGTTTGGAGCTAACAGTACC	this work	
		reverse	GAGGACAACGCAAATAAACATCCG		
AtBIP2	AT5G42020	forward	TTGCAGAGGAAGACAAGAAGGTG	this work	
		reverse	CACGTATGTCTCCAGGGCATTC		
AtBIP3	AT1G09080	forward	CACGGTTCCAGCGTATTTCAAT	Liu *et al.* , 2007b	https://doi.org/10.1105/tpc.106.050021
		reverse	ATAAGCTATGGCAGCACCCGTT		
AtSDF2	AT2G25110	forward	TCAAGAGTGGAGCAACCATTAG	Afrin *et al.* , 2020	https://doi.org/10.1038/s41598-020-76114-1
		reverse	CCAAAGCAGCTAACCTCTAAGT		
AtERDJ3A	AT3G08970	forward	GGTAGCTCATCGAATGCTGAA	Afrin *et al.* , 2020	https://doi.org/10.1038/s41598-020-76114-1
		reverse	GGTCCACAACGTCCTTCTTATAG		
AtERDJ3B	AT3G62600	forward	CAAATACGAACGGGAGGGATAC	Afrin *et al.* , 2020	https://doi.org/10.1038/s41598-020-76114-1
		reverse	GGTTCGCCGTCTTCATAGAAA		
AtPLP2	AT2G26560	forward	GTAGCTGGTTGGGGACTATTGA	La Camera *et al.* , 2005	https://doi.org/10.1111/j.1365-313X.2005.02578.x
		reverse	CGGTAGCGATATCAACAGAAGC		
AtPR1	AT2G14610	forward	AAGGGTTCACAACCAGGCAC	Anderson *et al.* , 2004	https://doi.org/10.1105/tpc.104.025833
		reverse	CACTGCATGGGACCTACGC		
AtPDF1.2a	AT5G44420	forward	TTTGCTGCTTTCGACGCAC	Anderson *et al.* , 2004	https://doi.org/10.1105/tpc.104.025833
		reverse	CGCAAACCCCTGACCATG		
AtNAC053/AtNTL4	AT3G10500	forward	TGTTGGGTGCTATTCCTGCT	Gladman *et al.* , 2016	https://doi.org/10.1105/tpc.15.01022
		reverse	CTGATGATTGTGCTGCGTGT		
AtNAC078/AtNTL11	AT5G04410	forward	TTGAAGAAAGCTGGTGTGCC	Gladman *et al.* , 2016	https://doi.org/10.1105/tpc.15.01022
		reverse	CCAGATTTTCGGGCTTCTCG		
AtANAC089/AtNTL14	AT5G22290	forward	GCCAACACTAGAATCAGCATCA	Ai *et al.* , 2021	https://doi.org/10.1111/tpj.15425
		reverse	TTGCTATCAGAGCCACTACACC		
AtCATHB1	AT1G02300	forward	CCACGGTGTAGTAACCCAAGA	Cai *et al.* , 2017	https://doi.org/10.1111/nph.14676
		reverse	GTATGCGCCGACACCATAG		
AtCATHB2	AT1G02305	forward	GTGTTAGCGGAAACCAGCTT	Cai *et al.* , 2017	https://doi.org/10.1111/nph.14676
		reverse	CAGTGAAGGCAACCTCAACA		
AtCATHB3	AT4G01610	forward	GAAATGCGTTAGCGACAACA	Cai *et al.* , 2017	https://doi.org/10.1111/nph.14676
		reverse	CTGCCATGATATCTTGTGGATT		